

Optically pumped AlGa_N quantum-well lasers at sub-250 nm grown by MOCVD on AlN substrates

Yuh-Shiuan Liu¹, Zachary Lochner¹, Tsung-Ting Kao¹, Md. Mahbub Satter¹, Xiao-Hang Li¹, Jae-Hyun Ryou^{1,2}, Shyh-Chiang Shen¹, P. Douglas Yoder¹, Theeradetch Detchprohm¹, Russell D. Dupuis^{1,*}, Yong Wei³, Hongen Xie³, Alec Fischer³, and Fernando Ponce³

¹ Center for Compound Semiconductors and School of Electrical and Computer Engineering, Georgia Institute of Technology, Atlanta, GA 30332-0250, USA

² Now at: Department of Mechanical Engineering, University of Houston, Houston, TX 77004, USA

³ Department of Physics, Arizona State University, Tempe, AZ 85287-1504, USA

Received 14 June 2013, accepted 13 November 2013

Published online 16 January 2014

Keywords AlGa_N, lasers, metalorganic chemical vapor deposition, MOCVD, III-nitride semiconductors

* Corresponding author: e-mail dupuis@gatech.edu, Phone: +1 404 385 6094, Fax: +1 404 385 6096

In this study, we employed bulk (0001) AlN substrates for the metalorganic chemical vapor deposition growth of AlGa_N multi-quantum-well heterostructures in an Aixtron 6 × 2" close-coupled showerhead reactor. The wafers were fabricated into cleaved bars with a cavity length of ~1 mm. Two different layer structure designs are presented in this work. Both laser bars were optically

pumped by a pulsed 193 nm ArF excimer laser at room temperature. The lasing wavelengths are 243.5 nm and 245.3 nm with threshold power density 427 kW/cm² and 297 kW/cm², respectively. Both laser bars showed transverse electric-polarization-dominated optical emission when operating above threshold.

© 2014 WILEY-VCH Verlag GmbH & Co. KGaA, Weinheim

1 Introduction Ultraviolet (UV) semiconductor light emitters have recently become of interest for a number of applications including water purification, food sanitation, bio-agent detection, optical memory storage, and medical sterilization [1, 2]. Mature UV light sources such as dye lasers, quadruple Nd:YAG, and excimer lasers suffer from several disadvantages including, containing toxic materials, a large footprint, high power consumption, and extreme fragility. Thus, a compact and efficient semiconductor-based alternative is desirable. The wide-bandgap III-nitride material system, specifically AlN and its composites: AlGa_N and AlInGa_N, can access the entire ultraviolet spectral range including near (320–400 nm), middle (280–320 nm), and deep-UV (200–280 nm) [3–7]. A deep-UV laser diode is a particularly sought after goal; however stimulated emission has been elusive due to the technical challenges that arise as the bandgap is widened with increasing aluminium mole fraction, such as lower free-carrier concentrations and higher defect densities. In addition, as the lasing wavelength decreases, the threshold power for laser

action increases due to the rate of spontaneous emission increases as $1/\lambda^3$. Thus, to the best of our knowledge, there has been no previous report of a DUV current injection laser diode (LD). On the other hand, optically pumped AlGa_N multi-quantum well (MQW) structures grown on SiC substrate with wavelength in sub-250 nm region was reported in 2004, but the threshold power density was as high as 1.2 MW/cm² [8].

More recently, various AlGa_N-based optically pumped lasers with lasing wavelength between 260 nm and 300 nm were reported [6, 9, 10]; however, the development in sub-250 nm DUV lasers are still rarely reported. In this study, *c*-plane AlN substrates were used for AlGa_N-based optically pumped sub-250 nm DUV lasers growth. Advantages for growth on a native substrate enables homoepitaxial growth for the buffer layer [11], which significantly reduces the density of dislocations in epitaxial layers and the subsequent active region growth. In addition, reducing the differences in thermal expansion of materials eliminates cracks formation during the thermal cycle and cool-down.

2 Experimental procedures Prior to growth, the AlN substrates were etched in a 3:1 H_2SO_4 : H_2PO_4 solution at 90°C for removing the native surface hydroxide [11]. The wafer is then annealed in a high-purity ammonia ambient at high temperature for the optimal epitaxial-ready condition. The epitaxial growth was done in an Aixtron $6 \times 2''$ close-coupled showerhead (CCS) metalorganic chemical vapour deposition (MOCVD) reactor. Due to low adatom mobility of Al atoms on the growing surface, high temperature and low V/III ratio are required for two-dimensional growth and smooth surface formation [12]. In this work, the relatively high growth temperature of 1130°C was used while the V/III ratios for AlN buffer layer and active region growth are set to less than 100 and approximately 400, respectively. The ideal temperature range for high aluminium mole fraction of AlGaIn-based material could be above 1200°C ; however, the limitations of this reactor prevent us from performing such high temperature growth.

Two epitaxial structures presented in this work are designed specifically for 193 nm pulsed ArF optical pumping. Sample 1-2651-5 has a 10-period of MQW as active region, with 3 nm $\text{Al}_{0.60}\text{Ga}_{0.40}\text{N}$ wells and 5 nm $\text{Al}_{0.75}\text{Ga}_{0.25}\text{N}$ barriers, between a 200 nm AlN regrowth buffer layer and a 10 nm AlN cap layer. On the other hand, sample 1-2693-2 has identical buffer layer, but different active layer design. Instead of 10 periods of MQW structure, which has 3 nm $\text{Al}_{0.60}\text{Ga}_{0.40}\text{N}$ wells and 6 nm $\text{Al}_{0.75}\text{Ga}_{0.25}\text{N}$ barriers, an 8-period MQW is used instead and capped by 8 nm of AlN. The thin AlN cap layer serve as a surface passivation layer and a cladding layer as well. Increasing the thickness of the cap layer would result a symmetric waveguide, which centers the optical mode at the active region and increase the optical confinement factor (Γ). However, the absorption loss of the 193 nm excitation source in the cap layer prohibits us to increase the thickness of the AlN cap layer.

After the growth, the wafers were thinned to $80\ \mu\text{m}$ by chemical-mechanical polishing the AlN substrate. Fabry-Perot cavities were formed by cleaved along m -plane facets with a cavity length 1.23 mm and 1.45 mm for sample 1-2651-5 and 1-2693-2, respectively. Neither high-reflection nor anti-reflection coatings were applied on the laser bars. Instead, the laser bars were directly optically pumped from the top surface by an ArF excimer laser ($\lambda_p = 193\ \text{nm}$) at a 10 Hz repetition rate with a pulse width of 20 ns. Figure 1 shows a schematic diagram of the experimental setup for optical pumping measurements. The laser beam from the pump laser passed through an optical aperture with the exit window $0.1\ \text{cm}$ by $1.27\ \text{cm}$ and illuminated the surface of laser bars. Attenuators were inserted to vary the pumping power density and a Glan-Laser α -BBO polarizer with 100,000:1 extinction ratio was used to measure the polarization of optical emission. An optical fiber was placed in the proximity of the laser facet for collecting optical output from laser bars. Optical emission spectra were analysed by an Ocean Optics Maya Pro spectrometer with a spectral resolution of $0.1\ \text{nm}$.

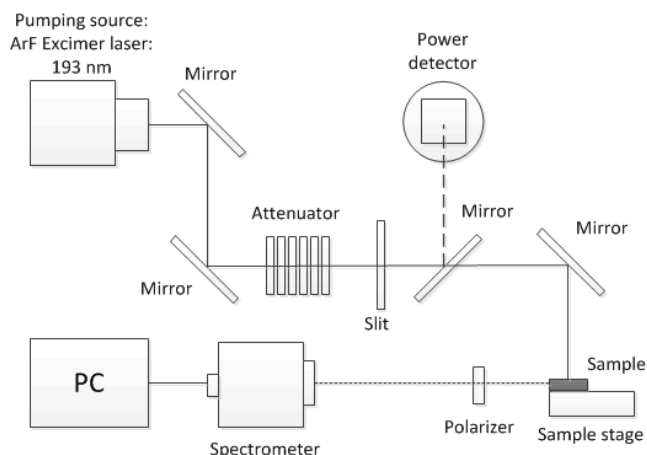


Figure 1 Experimental setup for optical pumping measurement system.

3 Results and discussion The optical emission spectra recorded at room temperature with various pumping power densities are shown in Fig. 2. The peak emission wavelengths were $\lambda = 243.5\ \text{nm}$ and $\lambda = 245.3\ \text{nm}$ for sample 1-2651-5 and 1-2693-2, respectively. Spectral linewidth narrowing with increasing in pumping power density was observed from both samples. Figure 3 shows the optical output power as a function of excitation power density (L - L curve) and the characteristic lasing threshold power densities (P_{th}) are determined to be $427\ \text{kW}/\text{cm}^2$ and $297\ \text{kW}/\text{cm}^2$ for sample 1-2651-5 and 1-2693-2, respectively. Stimulated emission output power increases linearly with the excitation power density beyond the threshold as demonstrated in Fig. 3. Notice the 30% threshold power density reduction in sample 1-2693-2 originated from the reduction in cap layer thickness and smaller active region.

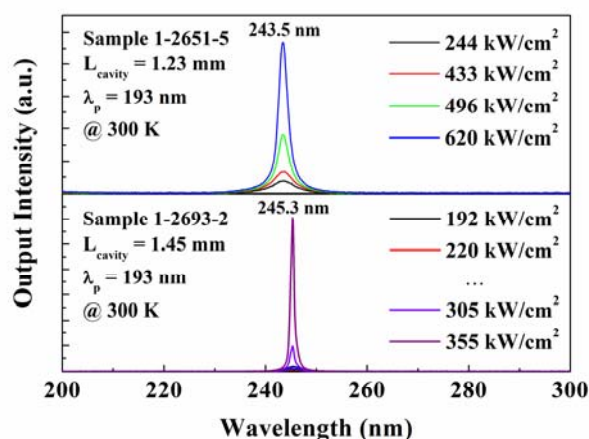


Figure 2 Optical emission spectra recorded at room-temperature at various excitation power density for sample 1-2651-5 (top panel) and samples 1-2693-2 (bottom panel).

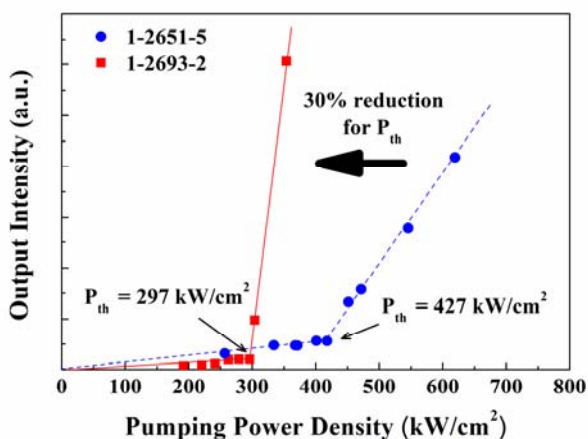


Figure 3 Optical output intensity as a function of excitation power density for sample 1-2651-5 (circles) and samples 1-2693-2 (squares). The improved layer design shows 30% reduction in threshold power density.

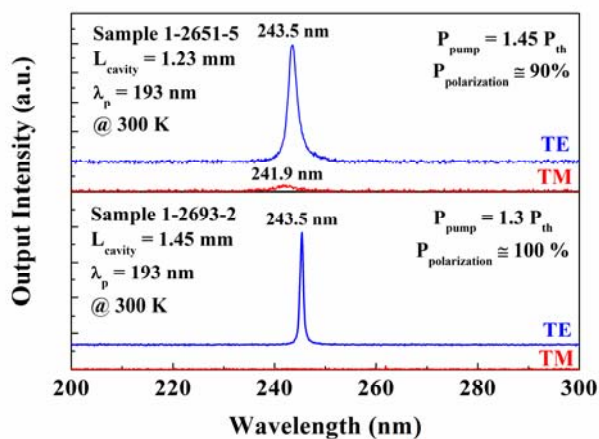


Figure 4 Optical emission spectra for both TE and TM polarizations recorded at room temperature above threshold power density for sample 1-2651-5 (top panel) and samples 1-2693-2 (bottom panel). An offset was applied on TE emission spectra in both panels for visual clarity.

However, reducing the total thickness of active region also reduces the total thickness of high index layers, which results reduction in the optical mode confinement factor. In order to solve the problem, quantum barrier thickness is increased to ensure a similar optical confinement factor.

Emission spectra for both transverse electric (TE) and transverse magnetic (TM) polarizations recorded above threshold power density are shown in Fig. 4. Both samples show strongly TE polarized with the degree of polarization ($P_{polarization}$), defined as $P_{polarization} = (I_{TE} - I_{TM}) / (I_{TE} + I_{TM})$, greater than 90%. In addition, the emission spectra for TM mode shows 1.6 nm shorter in peak wavelength compared to TE mode from sample 1-2651-5. Polarization measurement results presented in this work and in Refs. [6, 9, 13],

and [14] suggest the TE-mode gain continue to dominate in DUV for AlGaIn-based material.

4 Conclusion Stimulated emission from optically pumped AlGaIn-based DUV MQW lasers grown by MOCVD have been described. The native substrates allow better crystalline quality and results the significant reduction in threshold power density for sub-250 nm lasers. Improvements in epitaxial structure design also demonstrated further reduction in threshold power density. These results suggest the possibility to realize DUV electrical injection LD.

Acknowledgements This work is supported by the Defence Advanced Research Projects Agency under Contract FA2386-10-1-4152. RDD acknowledges additional support of the Steve W. Chaddick Endowed Chair in Electro-Optics and the Georgia Research Alliance.

References

- [1] T. D. Cutler and J. J. Zimmerman, *Anim. Health Res. Rev.* **12**, 15-23 (2011).
- [2] D. A. Parthenopoulos and P. M. Rentzepis, *Science* **245**, 843-845 (1989).
- [3] P. J. Parbrook and T. Wang, *IEEE J. Sel. Top. Quantum Electron.* **17**, 1402 (2011).
- [4] A. Fujioka, T. Misaki, T. Murayama, Y. Narukawa, and T. Mukai, *Appl. Phys. Express* **3**, 041001 (2010).
- [5] S. Fujikawa and H. Hirayama, *Appl. Phys. Express* **4**, 061002 (2011).
- [6] T. Wunderer, C. L. Chua, Z. Yang, J. E. Northrup, N. M. Johnson, G. A. Garrett, H. Shen, and M. Wraback, *Appl. Phys. Express* **4**, 092101 (2011).
- [7] W. H. Sun, J. P. Zhang, V. Adivarahan, A. Chitnis, M. Shatalov, S. Wu, V. Mandavilli, J. W. Yang, and M. A. Khan, *Appl. Phys. Lett.* **85**, 531-533 (2004).
- [8] T. Takano, Y. Narita, A. Horiuchi, and H. Kawanishi, *Appl. Phys. Lett.* **84**, 3567-3569 (2004).
- [9] J. Xie, S. Mita, Z. Bryan, W. Guo, L. Hussey, B. Moody, R. Schlessler, R. Kirste, M. Gerhold, R. Collazo, and Z. Sitar, *Appl. Phys. Lett.* **102**, 171102-171104 (2013).
- [10] V. N. Jmerik, E. V. Lutsenko, and S. V. Ivanov, *Phys. Status Solidi A* **210**, 439-450 (2013).
- [11] A. Rice, R. Collazo, J. Tweedie, R. Dalmau, S. Mita, J. Xie, and Z. Sitar, *J. Appl. Phys.* **108**, 043510 (2010).
- [12] H. J. Kim, S. Choi, D. Yoo, J.-H. Ryou, R. D. Dupuis, R. F. Dalmau, P. Lu, and Z. Sitar, *Appl. Phys. Lett.* **93**, 022103 (2008).
- [13] T. Wunderer, C. L. Chua, J. E. Northrup, Z. Yang, N. M. Johnson, M. Kneissl, G. A. Garrett, H. Shen, M. Wraback, B. Moody, H. S. Craft, R. Schlessler, R. F. Dalmau, and Z. Sitar, *Phys. Status Solidi C* **9**, 822 (2012).
- [14] W. W. Chow and M. Kneissl, *J. Appl. Phys.* **98**, 114502 (2005).